Front. Eng. Manag. 2019, 6(3): 351–367
https://doi.org/10.1007/s42524-019-0023-6

RESEARCH ARTICLE

Hongying ZHAO, Rebecca YANG, Chaohong WANG, W. M. Pabasara U. WIJERATNE, Chengyang LIU, Xiaolong XUE, Nishara ABDEEN

Effects of design parameters on rooftop photovoltaic economics in the urban environment: A case study in Melbourne, Australia

Abstract Many researchers found high potential of adopting building photovoltaic (PV) systems in urban areas, especially on building rooftop, to improve the sustainability of urban environment. However, the optimal energy output performance and economic benefit of the PV system are affected by the usable roof area, PV array layout, and shading effect considering high city density. This study aims to understand the effects of these design parameters in the urban environment of rooftop PV's economic performance. This study carries out a case study in the urban area of Melbourne with 90 PV designs under three shading conditions to generate 270 scenarios. Through a lifecycle cost-benefit analysis, including net present value (NPV), NPV per kW, internal return rate (IRR), and payback year, the results can help in developing a comprehensive understanding of the economic performance of rooftop PV designs that cover most of the urban areas of Melbourne. The optimal PV design scenarios for the urban environment are identified, thereby providing investors and industry professionals with useful information on value-for-money PV design. Meanwhile, the maximum shading loss that makes the PV systems financially unfeasible is investigated, and design scenarios with greatest ability to sustain the shading effect are identified. This research can also support the policy makers' decision on the development and deployment of the roof PV systems in urban planning.

Keywords building photovoltaics, tilt and azimuth, orientation, shading analysis, economic analysis

Received October 30, 2018; accepted January 26, 2019

Hongying ZHAO, Rebecca YANG (✉), W. M. Pabasara U. WIJERATNE, Chengyang LIU
School of Property, Construction and Project Management, Royal Melbourne Institute of Technology, Melbourne, Australia
E-mail: rebecca.yang@rmit.edu.au

Chaohong WANG
School of Architecture, Hebei University of Technology, Tianjin 300130, China

Xiaolong XUE
School of Business, Guangzhou University, Guangzhou 510006, China

Nishara ABDEEN
Department of Building Economics, University of Moratuwa, Moratuwa, Sri Lanka

1 Introduction

Increasing renewable energy sources (RESs) in the urban context is important to improve the sustainability of a city. Among all the available RESs, solar photovoltaic (PV) energy is one of the most promising candidates due to its continuous cost reduction and technological improvement (Freitas et al., 2018). Rooftop PV systems are extremely common in urban areas due to easy installation. A well-designed rooftop PV system cannot only exhibit considerable environmental benefit but also become an investment choice in adding value to building owners. However, many PV design parameters are constrained by the urban environment, which may cause considerable influences on the optimal energy output performance and economic benefit of rooftop PV systems. This study focuses on the tilt and azimuth angles of the PV system, usable roof area, and shading effect by the surrounding environment.

The tilt and azimuth angles of the PV arrays are the most important design parameters that have direct influences on obtaining solar irradiation and energy outputs (Jantsch et al., 1991; Bhattacharya et al., 2014; Singh and Banerjee, 2016). The common practice to simplify the PV array design is making the tilt angle equal to the geographic latitude and the azimuth angle equal to the due south in the northern hemisphere for a fixed PV array (Rowlands et al., 2011). Given that the solar condition differs based on the geographic location, a large amount of research has investigated the optimal tilt angle and azimuth angle for a certain location around the globe. For example, Khahro et al. (2015) identified the annual optimum tilt angle in the southern region of Sindh, Pakistan. The optimum tilt angle is 23°, which is slightly smaller than the local latitude (25°). Similar research can also be conducted in Saudi Arabia (Kaddoura et al., 2016), Turkey (Bakirci, 2012), and China's Taiwan (Chang, 2010). In addition to discovering the optimal tilt angle alone, many studies regarding the optimal setting of tilt and azimuth angles have been conducted to maximize the monthly or yearly energy yield, such as in Canada (Rowlands et al., 2011), Iran (Talebizadeh et al., 2011), and Abu Dhabi (Jafarkazemi and Saadabadi, 2013). Various models are established for the optimization of the PV system layout.

However, in terms of the rooftop PV design in urban areas, the possible effect of building orientation on the usable roof area for PV system is often neglected. Conflict may arise between the building orientation and the optimal PV array layout. In many cities, general building orientations are evident in urban blocks, which have been determined for decade by the metropolitan planning scheme. For example, in Melbourne, "Hoddle Grid" is the layout of streets in its central business district (CBD), which was established in 1837 and became the first formal town plan in the city (University of Melbourne, 2008; City of Melbourne, 2012). Two main building orientations are apparent in Melbourne. In this densely built district of Melbourne, most buildings are aligned with the layout of the streets, which is 20° counter-clockwise from true north. Most buildings outside the CBD are oriented at approximately 10° clockwise from true north (National Centers for Environmental Information, 2018). The capacity of a PV system is mainly affected by the number of PV panels placed on the available roof area. To achieve the maximum number of PV panels, researchers supposed that the orientation of the PV array, namely, the azimuth angle, is equal to the building orientation. However, the amount of annual solar irradiation varies depending on the azimuth angle. The general rule indicates that the surface facing due south achieves the most in the northern hemisphere and vice versa in the southern hemisphere (Mondol et al., 2007). Research on the economic assessment of the optimal design for rooftop PV in urban areas by considering both the main building orientations of the city and PV panel azimuth is limited.

Meanwhile, shading in the urban environment can have a larger influence on the PV system performance than any other design parameter (Horn, 2011). Shading is a major challenge imposed by surrounding obstruction, such as tall neighboring buildings or trees. In particular, in the urban environment, shading is becoming a major risk. As the cities increase in size, and buildings become tall, the likelihood of overshadowing buildings is high, which will result in considerable energy losses. Shading challenges can be the difference between a viable and a nonviable PV project. To guide the application of PV systems, many researchers investigated the solar potential of cities worldwide (Compagnon, 2004; Redweik et al., 2013; Sarralde et al., 2015; Mohajeri et al., 2016; Wong et al., 2016). Most studies evaluated the availability of solar irradiation under the effect of shading by the surrounding buildings through geographic information system-based methods (Melius et al., 2013). Some researchers analyzed the shading effects on the system yield and performance ratio reduction through experiment or by using a software (Zomer et al., 2014; Frontini et al., 2016; Zomer et al., 2016; Bana and Saini, 2017). However, research associating the shading effect to the economic performance of rooftop PV systems is lacking, especially in increasingly dense urban environment.

Considering the research gaps in the area, the main focus of this study is to investigate the effects of design parameters including the usable roof area, PV array layout, and shading ratio in the urban environment on rooftop PV's economic performance. This work carries out a case study in Melbourne, Australia with 90 PV designs under 3 proposed shading conditions to generate 270 scenarios. A life cycle cost-benefit analysis, including net present value (NPV), NPV per kW, and payback year (PB), is carried out to study the effects of shading, building orientation, and azimuth angle of a PV system. Meanwhile, a maximum shading loss that each PV system can withstand to remain financially feasible is identified through the economic analysis. The outcomes of the study can benefit both the investors and urban planners regarding the development and deployment of rooftop building PV in urban environment. This paper is organized as follows: Section 2 describes the research method, with detailed explanation on each investigation step, including design scenario development (Section 2.1), shading condition and maximum shading loss determination (Section 2.2), and cost-benefit analysis (Section 2.3); Section 3 presents the results and discussion; and Section 4 provides the conclusions and implications.

2 Method

The case building of this investigation belonged to an educational institute in the urban area of Melbourne, Australia. The total built-up area of this building was approximately 1131 m^2. Figure 1 illustrates the case building (in blue) in the selected urban block. As shown in Fig. 1, the surrounding environment of the case building can be considered as a typical example of modern urban environment, with high and low buildings around the case building. The height of the case building was approximately 6.9 m, while those of surrounding buildings varied

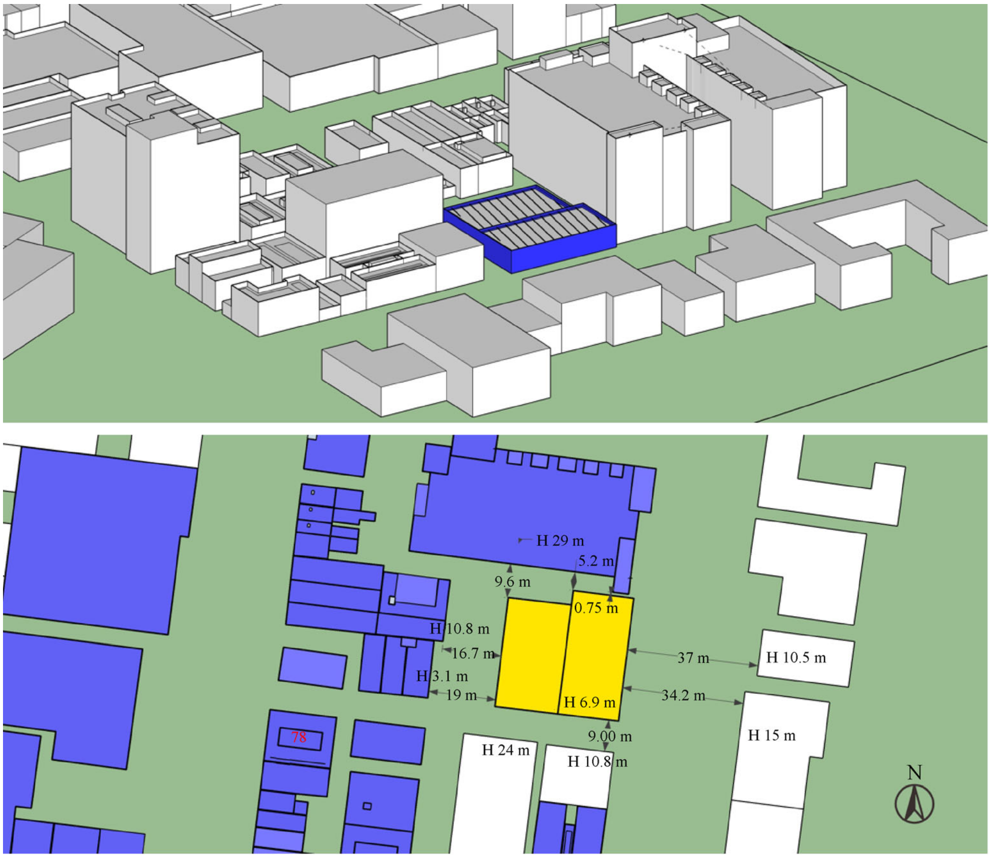

Fig. 1 3D modeling of case building and its surroundings

from 3.1 to 29 m. The case building was also selected because it had a regular rectangle shape, which aligned with the prevailing building designs. The shading condition of the selected areas was also analyzed and discussed in Section 2.2. The proposed PV systems were located on the roof of the case building. The design results are summarized in Appendix. Figure 2 provides an illustration of the PV design scenarios when the PV tilt angle was 38°.

Multiple data sources and tools were utilized in the study to carry out the economic analysis, as follows. (1) Building drawings and information were collected from the educational institute to create a SketchUp model of the case building and its surrounding environment. Google Earth was also used to assist the modeling process. (2) The detailed information of the selected PV module was obtained from a third-party PV design firm in Melbourne, who can provide the professional industry knowledge to the designs. (3) A total of 90 scenarios of PV layouts were proposed through the Skelion, which is a SketchUp plugin software with expertise in PV system design in 3D modeling. The explanation of the design process was provided in Section 2.1. Meanwhile, three different shading conditions were developed for the study (Section 2.2). (4) After the PV designs were developed, PV suppliers and installers were approached to obtain the capital cost information. A local utility provider advised the electricity price, and the feed-in-tariff (FIT) was obtained from the government website. (5) The hourly building consumption data were provided by the building owner. (6) Solar irradiation data were obtained from the NREL's PVWatts Calculator (NREL, 2018), which was used for energy output calculation. (7) Energy outputs were calculated based on the solar irradiation, system efficiency, and loss. Energy consumption and output data were compared to identify the possible energy export to the public grid. (8) The NPV, NPV per kW, and PB year were calculated to show the economic performance of all the designs. The design scenario with the best or worst economic performance was identified. (9) The maximum shading loss was calculated for each design scenario when the NPV became negative.

2.1 Developing design scenarios

When establishing the rooftop PV design, the present study considered the building orientation and the tilt angle and azimuth angle of the PV system. On the one hand, this study attempted to investigate the relationship between the

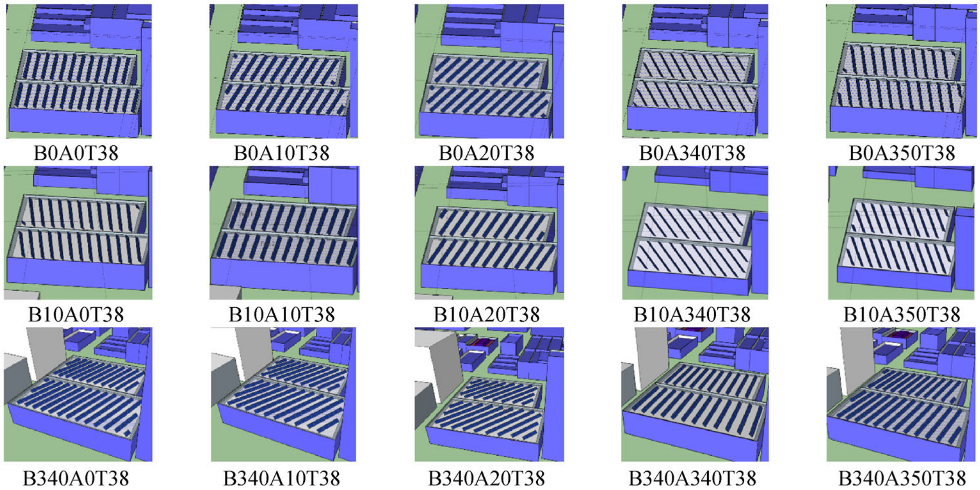

Fig. 2 3D models for PV design scenarios when the tilt angle was 38°. Note: B stands for the building orientation; A stands for the azimuth angle of the PV arrays; T stands for the tilt angle of the PV arrays

building orientation and the PV panel orientation (azimuth) to maximize usable roof area. On the other hand, this study aimed to discover the optimal setting of PV tilt and azimuth angles in Melbourne. In this study, an orientation/azimuth angle of 0° means north facing, and an orientation/azimuth angle of 90° is for true east.

The building orientation was classified as true north (0), 10° clockwise from true north (10), and 20° counter-clockwise from true north (340). The two classifications, namely, 10° clockwise from true north (10) and 20° counter-clockwise from true north (340), were included to align with the typical building orientations in Melbourne. In the SketchUp model, the orientation of the case building was changed, while the surrounding environment remained constant.

Regarding the azimuth angle of the PV design, we chose five sets of azimuth angle (i.e., from 20° counter-clockwise from true north (340) to 20° clockwise from true north (20)). The maximum PV usage area can be achieved when the building orientation was equal to the azimuth angle of the proposed PV system.

Six tilt angles were proposed (i.e., from 10° to 60°). For each building orientation, 30 alternative design scenarios were developed to determine the effects of tilt and azimuth angles on the economic performance of rooftop PV systems, as shown in Table 1. These combinations of tilt and azimuth angles were selected based on the study of the Australian Clean Energy Council (Clean Energy Council, 2009), as shown in Table 2. Instead of using a tilt angle of 40°, 38° was applied in the study, which was close to 40° and equal to the geographic latitude of Melbourne. Appendix provides a summary of all the design results in the study, where B represents building orientation, and A and T stand for the PV azimuth and tilt angles, respectively. For example, B0A0T10 indicates the combination of the building facing the true north, the PV azimuth angle of 0°, and the tilt angle of 10°. This setting remained the same throughout this study. These 90 design scenarios can help in developing a relatively comprehensive understanding of the rooftop PV design that covers the most urban areas of Melbourne.

The PV system design of each scenario was made with the principle to install as many PV panels as possible. The 90 scenarios of PV layouts were proposed through the Skelion. A popular polycrystalline silicon PV product was selected for the application, and the specification of the PV module input in the software is presented in Table 3. The distance for all the scenarios was set to guarantee that all PV panels can achieve at least 6 h of sunlight during winter solstice. According to PV selection and distance setting, the design results generated by the software are summarized in the Appendix to investigate the relationship between the building orientation and PV panel orientation (azimuth). The design results are discussed in Section 3.

2.2 Shading condition and maximum shading loss determination

The shading effect on the PV system in many studies refers to the solar irradiance or generation loss due to shading effect, which is generally in the form of percentage (Woyte et al., 2003; Loulas et al., 2012; Nguyen and Pearce, 2012). Nguyen and Pearce (2012) investigated the shading effect at the municipal scale in downtown Kingston, Ontario and showed that shading leads to a 25% generation loss in the average for > 12 months. Loulas et al. (2012) studied the shading loss of rooftop PV system on a building block in Greece. According to the study of Loulas et al. (2012), the annual performance loss due to shading varies from approximately 8% to 23%. A similar investigation on the

Table 1 Thirty design scenarios on the basis of tilt and azimuth angles

Azimuth angle/(°)	Design scenarios					
	10°	20°	30°	38°	50°	60°
0	A0T10	A0T20	A0T30	A0T38	A0T50	A0T60
10	A10T10	A10T20	A10T30	A10T38	A10T50	A10T60
20	A20T10	A20T20	A20T30	A20T38	A20T50	A20T60
340	A340T10	A340T20	A340T30	A340T38	A340T50	A340T60
350	A350T10	A350T20	A350T30	A350T38	A350T50	A350T60

Table 2 Annual daily irradiation on different plane inclination expressed as percentage of maximum value (source: Clean Energy Council, 2009)

Plane azimuth/(°)	Annual daily irradiation									
	0°	10°	20°	30°	40°	50°	60°	70°	80°	90°
0	86%	93%	98%	100%	100%	98%	93%	86%	77%	67%
10	86%	92%	97%	99%	99%	97%	92%	85%	77%	67%
20	86%	92%	96%	99%	98%	96%	91%	84%	76%	67%
30	86%	92%	95%	97%	96%	94%	89%	83%	75%	66%
40	86%	91%	94%	95%	95%	92%	87%	81%	74%	65%
340	86%	92%	97%	99%	99%	97%	93%	86%	78%	68%
350	86%	93%	98%	100%	100%	98%	93%	87%	78%	67%

Table 3 Specification of PV module used in the study

Feature	Description
Solar cell	156 mm×156 mm (6.1 in×6.1 in) polycrystalline silicon
No. of cells	60 (6×10)
Dimensions	1640 mm×992 mm× 35 mm (64.6 in×39.1 in×1.4 in)
Weight	18.2 kg (40.1 lb)
Front glass	3.2 mm (0.1 in) tempered glass
Frame	Anodized aluminum alloy
Junction box	IP67 rated (three bypass diodes)
Output cables	TUV (2Pfg1169:2007), UL 4703, UL44
	4.0 mm^2 (0.006 in^2), symmetrical lengths (–) 1000 mm (39.4 in) and (+) 1000 mm (39.4 in)
Connectors	MC4 connectors
Optimum operating voltage (V_{mp})	30.7 V
Optimum operating current (I_{mp})	8.15 A
Open circuit voltage (V_{oc})	37.4 V
Short circuit current (I_{sc})	8.63 A
Module efficiency	15.4%
Operating module temperature	–40 °C to +85 °C
Maximum power at STC (P_{max})	250 W

shading loss was carried out for the block where the case building is located, as shown in Fig. 3 (Yang and Carre, 2018). The result of this study showed that the average annual performance loss of rooftop PV system in this building block is 16%. Deline et al. (2012) also indicated that the annual shading losses in a typical urban

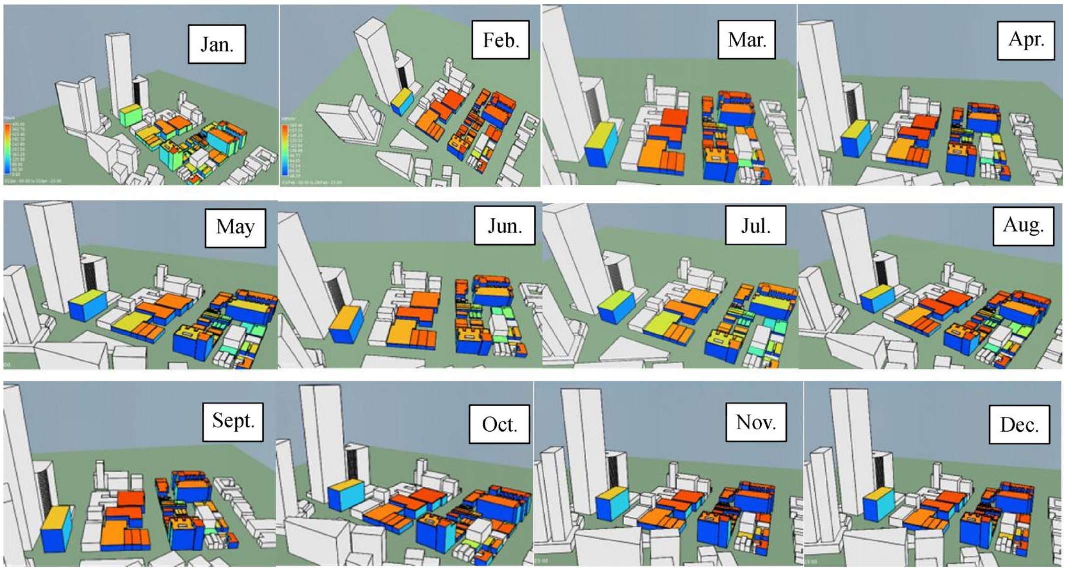

Fig. 3 Monthly solar irradiation value of the building block (Yang and Carre, 2018)

environment are 7%, 19%, and 25% under light, moderate, and heavy shading scenarios, respectively. Therefore, the present study adopts the three shading effect patterns not only to reflect on the current urban environment in Melbourne but also provide indications to urban developmental changes and other cities in Australia.

This study investigated a maximum shading loss that makes each design scenario financially unattractive (i.e., the NPV becomes negative) through the cost-benefit analysis. The results of maximum shading loss indicate the ability of each PV design scenario to sustain the shading loss in the urban environment.

2.3 Cost-benefit analysis

A 25-year cost-benefit analysis was carried out to study the actual value of all 90 PV designs under three shading conditions. The cost consists of the initial investment cost of each system and maintenance cost for 25 years. The cost information regarding the PV system was obtained from local PV suppliers and installers.

For the calculation of the benefit of the PV system, the first step was to calculate the energy output of the PV system by using Eq. (1), as follows:

$$E = A \cdot r \cdot H \cdot PR, \tag{1}$$

where E is the energy output in kW·h, A is the total solar cell area in m^2, which is equal to the number of PV panel in each system timing the area of PV cell on one PV panel, r is the PV product efficiency in percentage, H is the hourly solar radiation in kW·h/m^2, and PR is the system performance ratio.

The area of solar cell on the PV panel and the r of the PV panel used in the study are provided in Table 3. The corresponding H statistics that were used in each scenario were collected from a popular solar modelling tool named PVWatts (NREL, 2018). H represents the actual solar irradiation without additional effects on building shading. The shading loss in the study was applied on the PR, which was 90%×(1−Shading loss). The percentage in the equation, that is, 90%, is the system performance ratio provided by the PV supplier. Three shading losses, namely, 7%, 19%, and 25% for light, moderate, and heavy shading conditions, were examined, respectively. The attenuation rate of the PV system was assumed to be 0.7% per year for all the cases.

The second step was to compare the energy output with the building energy consumption. The building energy consumption of every 15 min interval was measured for 1 year. The hourly energy consumption data were generated from the original data and compared with the hourly energy output. If the energy output exceeds the building consumption, then the surplus energy will be sold to the public grid at the price of FIT set by the government.

The final equation of the benefit generated by the PV system is shown in Eq. (2). The detailed information used in the study is shown in Table 4.

$$B(n) = \sum\nolimits_{25} ep_n (1 + ep)^n E_1(h) + \text{FIT} \cdot E_2(h), \tag{2}$$

where n is the number of the year, ep_h is the electricity price of that h, Δep is the compounded growth rate of the electricity price of Melbourne calculated from the government report (Australian Energy Regulator, 2017), $E_1(h)$ is the hourly energy generation using Eq. (1) and consumed by the building, FIT is the FIT set by the government (State Government of Victoria, 2018), and $E_2(h)$ is the surplus

Table 4 Benefits of applying PV designs

Benefits	Values
Electricity rate	0.14 AUD per kW·h (0:00–7:00) 0.19 AUD per kW·h (7:00–24:00; Australian Energy Market Commission, 2017)
Electricity growth rate	5.42% per annum (Australian Energy Regulator, 2017)
Feed-in-tariff	0.113 AUD per kW·h (State Government of Victoria, 2018)

energy sold to the public grid. In this study, we assumed that the energy consumption of the case building remained the same for 25 years. However, with the increase in energy consumption in the future, the demand for additional solar energy for self-consumption will increase, thereby leading to a highly feasible solution to use PV. We presented a strict scenario here.

The NPV, NPV per kW, PB, and internal return rate (IRR) were selected for the cost-benefit analysis in the study. Equations (3) and (4) were used to calculate NPV and IRR in the study. The NPV per kW was applied in the following sections to compare each scenario with different PV capacities for the standardization of the comparison instead of NPV. PB is the number of years when the NPV becomes positive.

$$\mathrm{NPV} = -C_0 + \sum\nolimits_{n=1}^{N} \frac{B_n}{(1+r)^n} - \sum\nolimits_{n=1}^{N} \frac{M_n}{(1+r)^n}, \quad (3)$$

$$0 = -C_0 + \sum\nolimits_{n=1}^{N} \frac{B_n}{(1+\mathrm{IRR})^n} - \sum\nolimits_{n=1}^{N} \frac{M_n}{(1+\mathrm{IRR})^n}, \quad (4)$$

where C_0 is the initial investment cost, $B(n)$ is the benefit generated by the PV system using Eq. (2), M_n is the maintenance cost, which is assumed to be the cost of changing the invertors every 10 years, and r is the discount rate, which is assumed to be 7% in this study (Office of Best Practice Regulation, 2016).

3 Results and discussion

The results of the study are presented and discussed in this section. The three subsections are as follows: (1) the analysis of the design results to investigate the effects of building orientation and PV tilt and azimuth angles on the usable roof area, (2) economic performance of 90 different design scenarios under three shading conditions, and (3) maximum shading loss that makes the system financially unviable.

3.1 Analysis of 90 PV design results

From the geometrical perspective, the number of PV panels will reach its maximum when all panels are parallel to the building's orientation. However, as shown in Appendix, the design results indicated that the number of PV panels reached the maximum when the PV azimuth angle was 0° (i.e., facing north) regardless of the building orientation. When the PV arrays were parallel to the building orientation, scenario B10A10 had the second most PV panels among all five B10 scenarios, while scenario B340A340 possessed the second least panels among all five B340 scenarios. The finding was due to the distance between PV arrays. A suitable space should be provided between arrays to avoid shading effects among the arrays and guarantee that all PV panels can achieve at least 6 h of exposure to sunlight during winter solstice.

The results also showed that the number of PV panel decreased when the PV arrays had a large tilt angle setting. The largest number of PV panels for each set of building orientation and azimuth angle can be reached when the PV tilt angle was the smallest (10°) because the large tilt angle can increase the shading effects among the arrays, which required a large distance between the two adjacent PV panels, thereby reducing the number of PV panels.

3.2 Performance of proposed PV system designs under three shading conditions

The NPV, NPV per kW, and PB results of all the scenarios under three shading conditions are illustrated in Figs. 4–7. In general, the results of the economic indicators showed a consistent patent under three shading conditions. As shown in Fig. 4, among all building orientations, the T10 groups with the highest NPV and NPV decreased when the tilt angle increased. According to Figs. 5 and 7, NPV per kW and IRR reach their peaks when the tilt angle ranged from 30° to 38°. Meanwhile, the PV system demonstrated the shortest PB when the tilt angle was set from 20° to 50° under three shading conditions.

A summary table (Table 5) was generated to improve the comparison in terms of the performance of all 90 design scenarios. The table lists the best and worst design scenarios of the three shading conditions. The percentage difference between the two scenarios was also provided. In addition to all the economic indicators (i.e., NPV, NPV per kW, PB, and IRR), the total generation of the PV system and self-consumption ratio was included in the table to understand the economic results.

Regardless of the building orientation, A0T10 exhibited the best NPV, while A340T60 had the worst NPV under all three shading conditions. As shown in Appendix, the A0T10 of all three building orientations had the largest system capacity, thereby indicating that it possessed the largest area of the solar cells and highest initial investment cost. By contrast, the A340T60 of all three building orientations had the smallest or second smallest system capacity. As a result, B0A0T10, B10A0T10, and

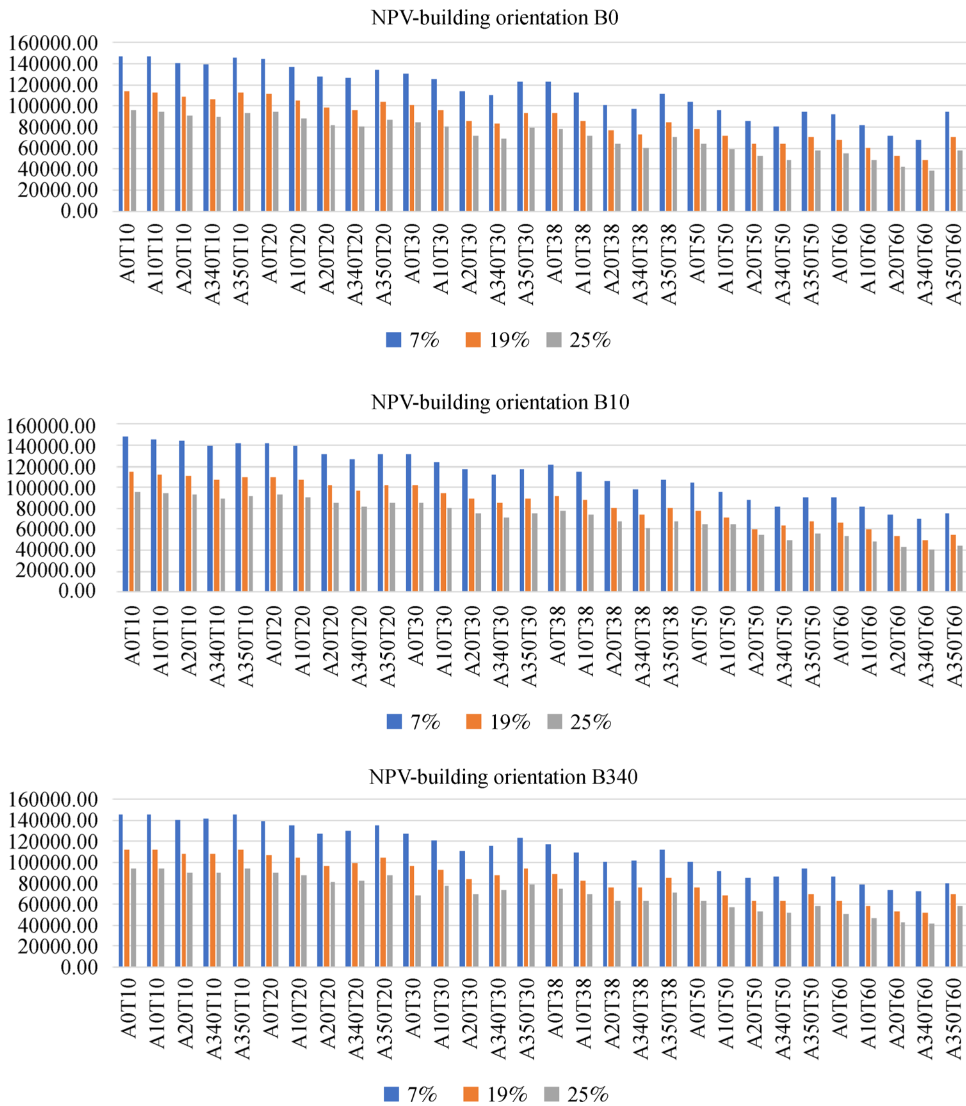

Fig. 4 NPV of all the scenarios under three shading conditions

B340A0T10 presented the highest 25-year energy output under three shading conditions, while B0A340T60 and B10A340T60 showed the least total energy generation during the entire lifespan. Although A0T10 had the highest energy generation, its self-consumption ratio was the lowest, thereby indicating that more surplus energy was sold to the public grid than the other design scenarios. A340T60 showed the opposite result with the least energy generation and almost 100% self-consumption ratio under all three shading conditions.

Given that the 90 scenarios had a variety of system capacities on the basis of the available roof areas, the NPV per kW can provide an improved understanding of the system benefit per unit. With regard to NPV per kW, the best scenarios for the three building orientations occurred when the PV azimuth angle was either 10° or 20°, and the title angle was equal to 20° or 38°. On the contrary, the combination of A0T10, A340T60, and A350T10 should be avoided for all three building orientations under different shading conditions due to the lowest NPV per kW. Meanwhile, the IRR performance was similar to that of NPV per kW.

In terms of PB, the difference among the scenarios under three shading conditions was insignificant. All scenarios can be breakeven in the 13th and 15th year under light and heavy shading conditions, respectively. The difference in PB between the best and worst scenarios was either 1 or 2 years.

3.3 Maximum shading loss

Considering the ongoing growth of urban environment, the maximum annual shading loss that resulted in the NPV of 0 was identified, as shown in Fig. 8. The maximum shading

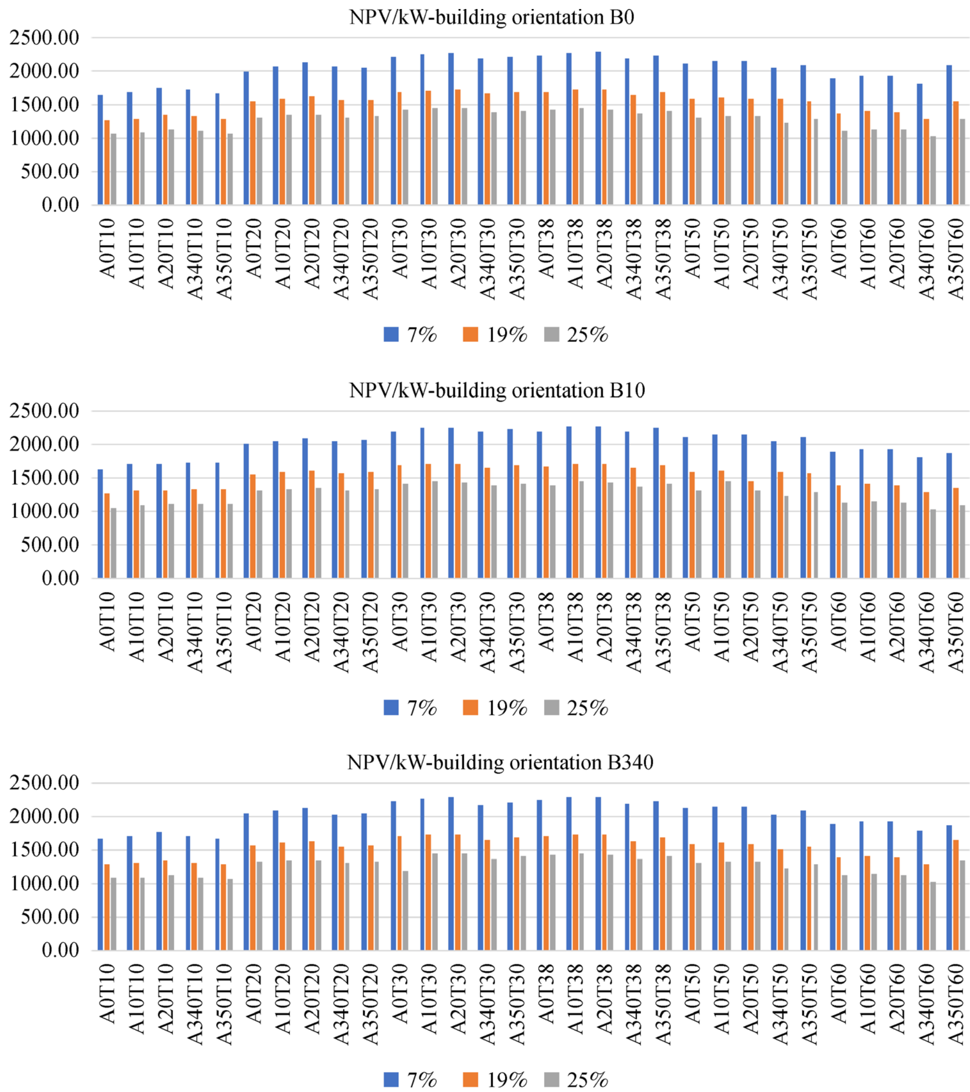

Fig. 5 NPV per kW of all the scenarios under three shading conditions

loss varied from 50% to 56%. As shown in Fig.8, for the three building orientations, A0T30, A10T30, A20T30, and A10T38 were the best designs to sustain the shading loss, while A340T60 was the worst. Although the PV design scenario reached the largest panel area and highest system capacity when the azimuth angle was 0°, the performance of these A0 scenarios was not the optimum when coping with shading loss. High solar irradiation instead of the large panel area made the system sustain substantial shading. As shown in Table 6, the average solar irradiation of the four best scenarios was approximately 4.83 $kW \cdot h \cdot m^{-2} \cdot d^{-1}$, which was the highest among all other angle combinations in this study (NREL, 2018). The result indicated that the combination of tilt and azimuth angles to obtain solar irradiation was the critical factor to deal with shading loss instead of building orientation.

4 Conclusions and implications

The solar PV system is one of the most promising RESs that can improve the sustainability of the urban environment. However, many design parameters are constrained by the urban context that can affect the PV system performance. This study investigates the effects of tilt and azimuth angles of the PV system, building orientation, and shading effect by the surrounding environment on the rooftop PV design for urban areas from the economic perspective. This work carries out a case study on the urban area of Melbourne. The 90 design scenarios are generated by considering both the building orientation and PV panel layout. The design results show that the combination of A0T10 for buildings of all three

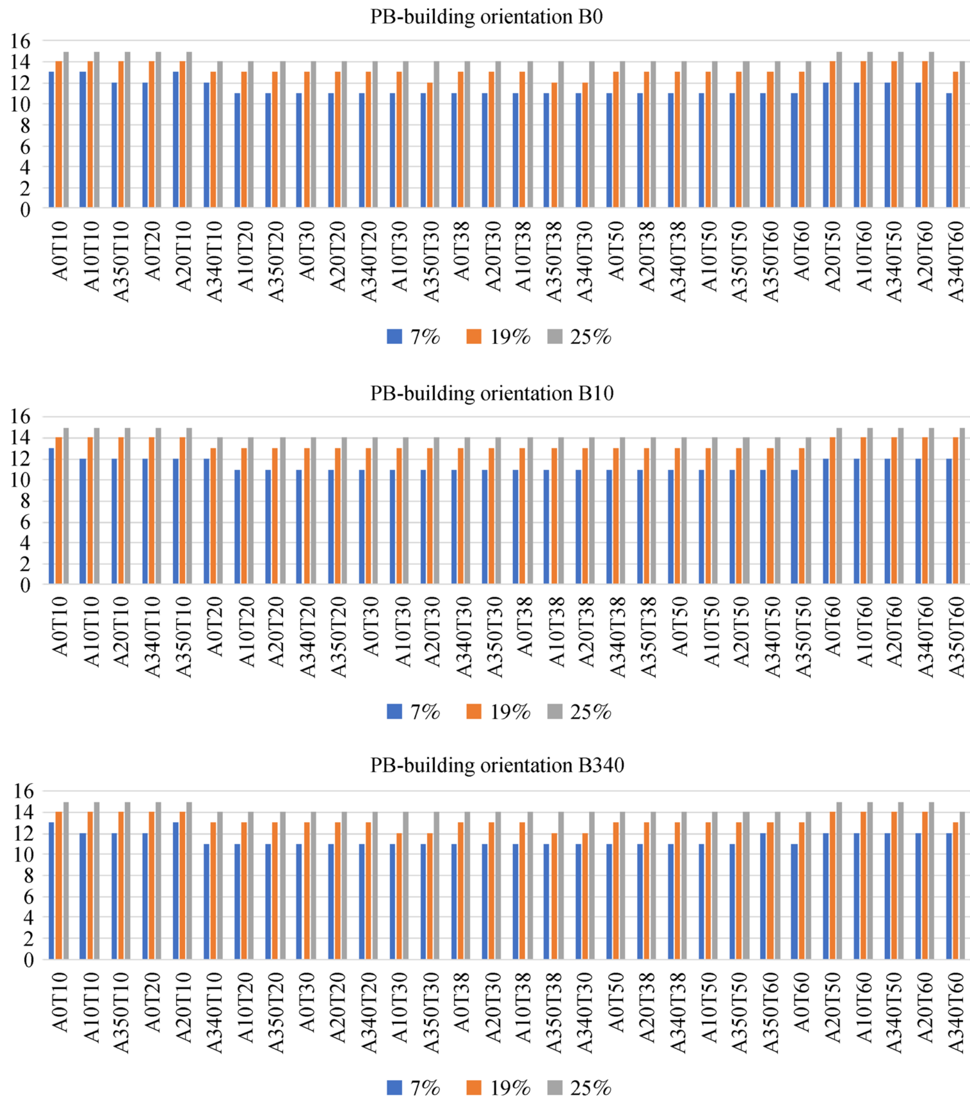

Fig. 6 PB of all the scenarios under three shading conditions

orientations in Melbourne can provide that largest panel area and system capacity.

A lifecycle cost-benefit analysis is conducted to investigate the economic performance of the 90 PV designs under three shading conditions, which generates 270 scenarios. NPV, NPV per kW, PB, and IRR are used to evaluate the economic performance of all the scenarios. The results of the economic analysis provide a comprehensive understanding of the economic performance of rooftop PV system design in the urban areas of Melbourne under different shading prospects. The best PV design scenarios for the urban environment are identified, thereby providing investors and industry professionals with useful information on the value-for-money PV design.

This study also identifies the value of maximum shading loss that makes the proposed PV systems financially unfeasible. The results show that the maximum shading loss varies from 50% to 56%. Regardless of the building orientation, the PV design combination of A0T30, A10T30, A20T30, and A10T38 has the optimal capability of sustaining overshadowing.

This research can also support policy makers' decision on the deployment of the roof PV systems in the urban areas. For the existing roof PV systems and envisioned PV projects, future urban development plans should consider the shading effects of buildings in the increasing high-density urban environment.

For building PV design, a large number of design parameters can affect the system performance and economic benefit (Wijeratne et al., 2018). This work has several limitations as a result of the case study. First, we only study the PV layout on the case building roof with a regular rectangular shape. The PV layout can be easily arranged when the building roof and PV module are rectangular in shape. However, the rectangular roof is the

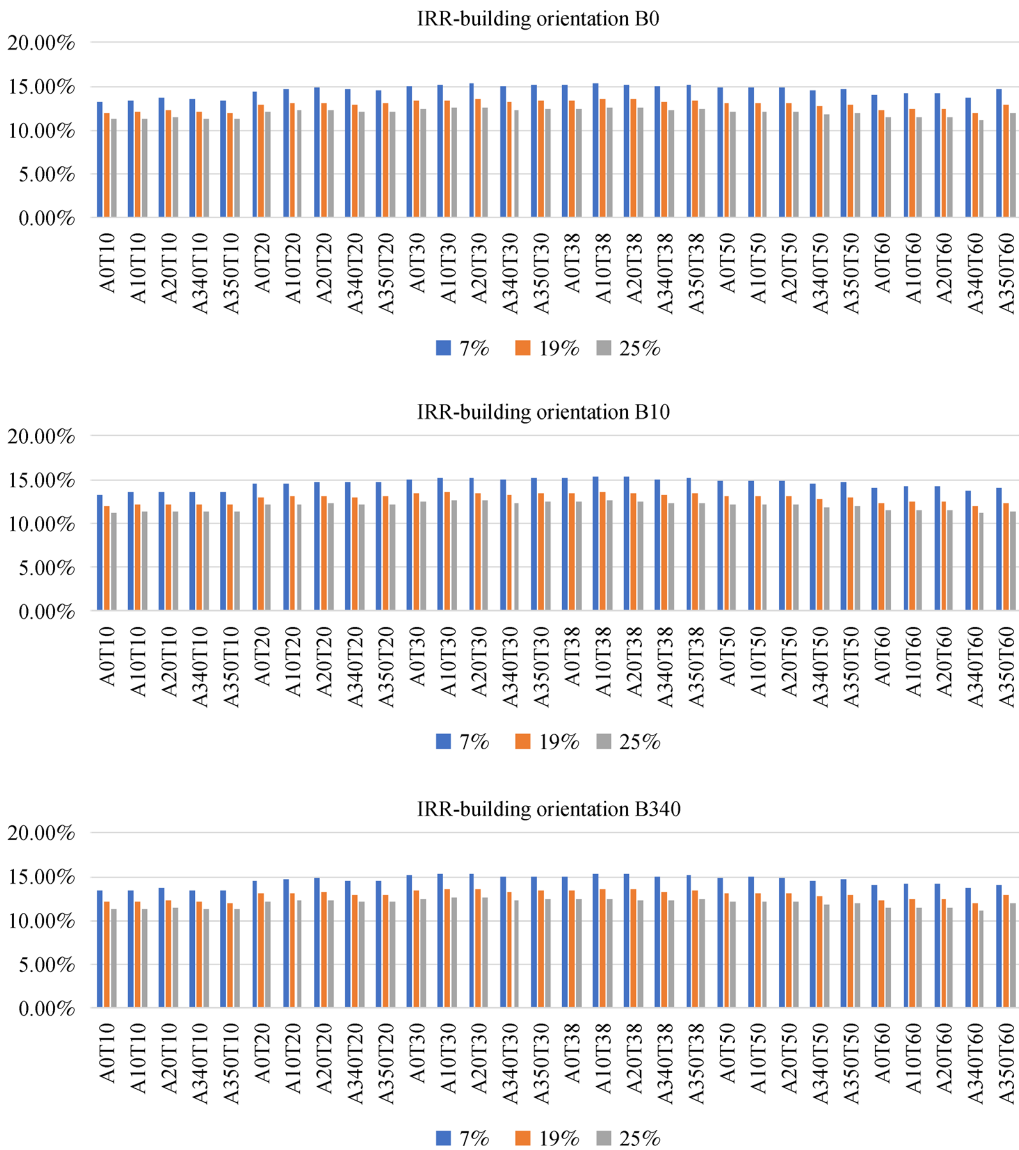

Fig. 7 IRR of all the scenarios under three shading conditions

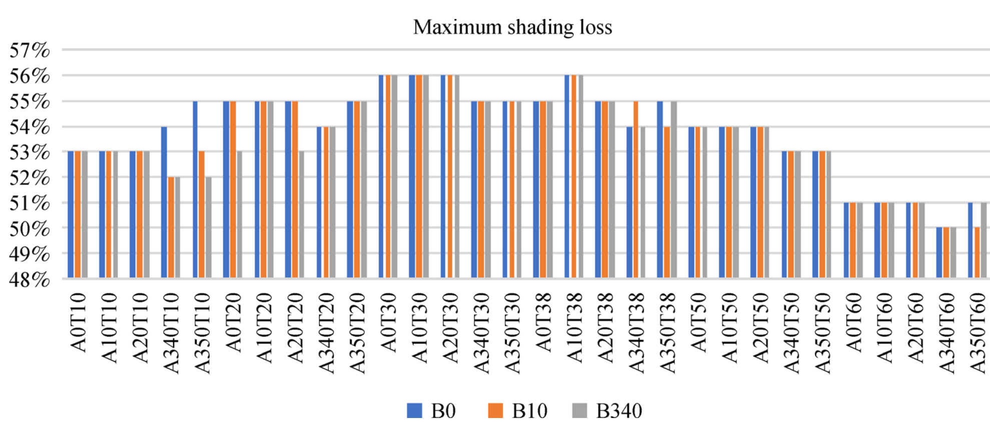

Fig. 8 Maximum annual shading loss of all the design scenarios

Table 5 Summary of the best and worst design scenarios under three shading conditions

Building orientation	Shading condition	Parameter	Best design		Worst design		Difference
			Design scenario	Value	Design scenario	Value	
B0	7%	NPV (7%) after 25 years	A0T10	147595	A340T60	67560	118.46%
		NPV per kW of system	A20T38	2287	A0T10	1658	37.93%
		Payback period (years)	–	11	A0T10	13	2 years
		IRR	A10T38	15.31%	A0T10	13.33%	14.85%
		Self-consumption ratio	A340T60	99.29%	A0T10	80.02%	24.08%
		Total energy generation	A0T10	2572243	A340T60	1002102	156.68%
	19%	NPV (7%) after 25 years	A0T10	113972	A340T60	48,489.	135.05%
		NPV per kW of system	A10T38	1733	A0T10	1281	35.31%
		Payback period (years)		13	–	14	1 year
		IRR	A10T38	13.53%	A0T10	12.00%	12.75%
		Self-consumption ratio	A340T60	99.78%	A0T10	85.57%	16.61%
		Total energy generation	A0T10	2240341	A340T60	872798	156.68%
	25%	NPV (7%) after 25 years	A0T10	95699	A340T60	38851	146.32%
		NPV per kW of system	A10T38	1452	A340T60	1043	39.19%
		Payback period (years)	–	14	–	15	1 year
		IRR	A10T38, A20T30	12.57%	A0T10	11.26%	11.63%
		Self-consumption ratio	A340T60	99.93%	A0T10	88.28%	13.20%
		Total energy generation	A0T10	2074390	A340T60	808147	156.68%
B10	7%	NPV (7%) after 25 years	A0T10	148280	A340T60	69712	112.70%
		NPV per kW of system	A20T38	2275	A0T10	1643	38.47%
		Payback period (years)	–	11	A0T10	13	2 years
		IRR	A20T38	15.29%	A0T10	13.28%	15.14%
		Self-consumption ratio	A340T60	99.13%	A0T10	79.44%	24.79%
		Total energy generation	A0T10	2608370	A340T60	1035729	151.84%
	19%	NPV (7%) after 25 years	A0T10	114565	A340T60	50074	128.79%
		NPV per kW of system	A10T38	1727	A0T10	1269	36.06%

(*Continued*)

Building orientation	Shading condition	Parameter	Best design		Worst design		Difference
			Design scenario	Value	Design scenario	Value	
		Payback period (years)	–	13	–	14	1 year
		IRR	A10T38	13.51%	A0T10	11.96%	12.96%
		Self-consumption ratio	A340T60	99.68%	A0T10	85.04%	17.22%
		Total energy generation	A0T10	2271806	A340T60	902087	151.84%
	25%	NPV (7%) after 25 years	A0T10	96218	A340T60	40140	139.71%
		NPV per kW of system	A10T50	1456	A340T60	1,043	39.62%
		Payback period (years)	–	14	–	15	1 year
		IRR	A10T30	12.57%	A340T60	11.13%	12.94%
		Self-consumption ratio	A340T60	99.87%	A0T10	87.82%	13.72%
		Total energy generation	A0T10	2103524	A340T60	8352656	151.84%
B340	7%	NPV (7%) after 25 years	A0T10	146267	A340T60	72689	101.22%
		NPV per kW of system	A20T38, A10T38	2289	A350T10	1677	36.51%
		Payback period (years)	–	11	A0T10, A350T10	13	2 years
		IRR	A10T38, A20T38	15.34%	A350T10	13.39%	14.56%
		Self-consumption ratio	A20T60	99.05%	A0T10	81.09%	22.15%
		Total energy generation	A0T10	2507215	A20T60	1061318	136.24%
	19%	NPV (7%) after 25 years	A0T10	112816	A340T60	522656	115.85%
		NPV per kW of system	A10T38	1737	A350T10	1292	34.49%
		Payback period (years)	–	12	–	14	2 year
		IRR	A10T38, A20T30	13.54%	A350T10	12.04%	12.46%
		Self-consumption ratio	A20T60	99.64%	A0T10	86.51%	15.18%
		Total energy generation	A0T10	2183703	A20T60	924374	136.24%
	25%	NPV (7%) after 25 years	A0T10	94687	A340T60	41927	125.84%
		NPV per kW of system	A10T30	1456	A340T60	1042	39.73%
		Payback period (years)	–	14	–	15	1 year
		IRR	A10T30	12.59%	A340T60	11.13%	13.12%
		Self-consumption ratio	A20T60	99.85%	A0T10	89.11%	12.05%
		Total energy generation	A0T10	2021947	A20T60	855902	136.24%

Table 6 Annual daily irradiation ($kW \cdot h \cdot m^{-2} \cdot d^{-1}$, source: NREL, 2018)

Azimuth angle	Annual daily irradiation/($kW \cdot h \cdot m^{-2} \cdot d^{-1}$)					
	T10	T20	T30	T38	T50	T60
A0	4.58	4.77	4.84	4.82	4.65	4.39
A10	4.59	4.78	4.85	4.83	4.66	4.41
A20	4.58	4.76	4.84	4.81	4.65	4.39
A340	4.54	4.70	4.75	4.71	4.52	4.26
A350	4.57	4.74	4.81	4.78	4.60	4.34

most popular roof shape in the case city. Hence, the results can be easily generalized. Second, the case building is an institutional building. Thus, the load profile and energy consumption data used in the study can only represent this kind of building. Third, we have not considered the potential change of energy consumption in the case building. However, if the building energy consumption increases, then the self-consumption ratio will increase, and the economic performance of the PV system will also improve. Finally, the shading effect is quantified by percentage values. Future research will explore the method to visualize shading loss, which can further facilitate the uptake and diffusion of rooftop PV system in the urban environment.

Appendix

Table A1 Summary of all 90 scenarios established by Skelion

Name	Building orientation/(°)	PV azimuth angle/(°)	PV tilt angle/(°)	Number of PV panels	System capacity/kW
B0A0T10	0	0	10	356	89.00
B0A10T10	0	10	10	347	86.75
B0A20T10	0	20	10	320	80.00
B0A340T10	0	340	10	320	80.00
B0A350T10	0	350	10	347	86.75
B10A0T10	10	0	10	361	90.25
B10A10T10	10	10	10	339	84.75
B10A20T10	10	20	10	334	83.50
B10A340T10	10	340	10	320	80.00
B10A350T10	10	350	10	329	82.25
B340A0T10	340	0	10	347	86.75
B340A10T10	340	10	10	340	85.00
B340A20T10	340	20	10	319	79.75
B340A340T10	340	340	10	330	82.50
B340A350T10	340	350	10	347	86.75
B0A0T20	0	0	20	288	72.00
B0A10T20	0	10	20	262	65.50
B0A20T20	0	20	20	241	60.25
B0A340T20	0	340	20	243	60.75
B0A350T20	0	350	20	262	65.50
B10A0T20	10	0	20	282	70.50
B10A10T20	10	10	20	271	67.75
B10A20T20	10	20	20	252	63.00
B10A340T20	10	340	20	246	61.50
B10A350T20	10	350	20	254	63.50
B340A0T20	340	0	20	271	67.75

(*Continued*)

Name	Building orientation/(°)	PV azimuth angle/(°)	PV tilt angle/(°)	Number of PV panels	System capacity/kW
B340A10T20	340	10	20	258	64.50
B340A20T20	340	20	20	239	59.75
B340A340T20	340	340	20	254	63.50
B340A350T20	340	350	20	264	66.00
B0A0T30	0	0	30	237	59.25
B0A10T30	0	10	30	222	55.50
B0A20T30	0	20	30	199	49.75
B0A340T30	0	340	30	199	49.75
B0A350T30	0	350	30	222	55.50
B10A0T30	10	0	30	240	60.00
B10A10T30	10	10	30	220	55.00
B10A20T30	10	20	30	208	52.00
B10A340T30	10	340	30	204	51.00
B10A350T30	10	350	30	211	52.75
B340A0T30	340	0	30	228	57.00
B340A10T30	340	10	30	214	53.50
B340A20T30	340	20	30	193	48.25
B340A340T30	340	340	30	212	53.00
B340A350T30	340	350	30	224	56.00
B0A0T38	0	0	38	220	55.00
B0A10T38	0	10	38	197	49.25
B0A20T38	0	20	38	177	44.25
B0A340T38	0	340	38	177	44.25
B0A350T38	0	350	38	199	49.75
B10A0T38	10	0	38	216	54.00
B10A10T38	10	10	38	203	50.75
B10A20T38	10	20	38	186	46.50
B10A340T38	10	340	38	178	44.50
B10A350T38	10	350	38	190	47.50
B340A0T38	340	0	38	209	52.25
B340A10T38	340	10	38	192	48.00
B340A20T38	340	20	38	175	43.75
B340A340T38	340	340	38	186	46.50
B340A350T38	340	350	38	201	50.25
B0A0T50	0	0	50	195	48.75
B0A10T50	0	10	50	177	44.25
B0A20T50	0	20	50	158	39.50
B0A340T50	0	340	50	158	39.50
B0A350T50	0	350	50	179	44.75
B10A0T50	10	0	50	197	49.25
B10A10T50	10	10	50	178	44.5
B10A20T50	10	20	50	163	40.75
B10A340T50	10	340	50	158	39.50
B10A350T50	10	350	50	171	42.75

(*Continued*)

Name	Building orientation/(°)	PV azimuth angle/(°)	PV tilt angle/(°)	Number of PV panels	System capacity/kW
B340A0T50	340	0	50	190	47.50
B340A10T50	340	10	50	170	42.50
B340A20T50	340	20	50	159	39.75
B340A340T50	340	340	50	169	42.25
B340A350T50	340	350	50	179	44.75
B0A0T60	0	0	60	195	48.75
B0A10T60	0	10	60	171	42.75
B0A20T60	0	20	60	149	37.25
B0A340T60	0	340	60	149	37.25
B0A350T60	0	350	60	179	44.75
B10A0T60	10	0	60	190	47.50
B10A10T60	10	10	60	169	42.25
B10A20T60	10	20	60	153	38.25
B10A340T60	10	340	60	154	38.50
B10A350T60	10	350	60	161	40.25
B340A0T60	340	0	60	181	45.25
B340A10T60	340	10	60	164	41.00
B340A20T60	340	20	60	153	38.25
B340A340T60	340	340	60	161	40.25
B340A350T60	340	350	60	170	42.50

Note: B means the building orientation; A and T indicate the azimuth and tilt angles of the PV arrays, respectively

References

Australian Energy Market Commission (2018). 2018 residential electricity price trends review. https://www.aemc.gov.au/sites/default/files/2018-12/2018%20Price%20Trends%20-%20Final%20Report%20-%20CLEAN.PDF, 2018-8-15

Australian Energy Regulator (2017). State of the Energy Market-May 2017. Performance Report

Bakirci K (2012). General models for optimum tilt angles of solar panels: Turkey case study. Renewable & Sustainable Energy Reviews, 16(8): 6149–6159

Bana S, Saini R P (2017). Experimental investigation on power output of different photovoltaic array configurations under uniform and partial shading scenarios. Energy, 127: 438–453

Bhattacharya P, Dey S, Mustaphi B (2014). Some analytical studies on the performance of grid connected solar photovoltaic system with different parameters. Procedia Materials Science, 6: 1942–1950

Chang Y P (2010). Optimal the tilt angles for photovoltaic modules in Taiwan. International Journal of Electrical Power & Energy Systems, 32(9): 956–964

City of Melbourne (2012). Thematic history: a history of the city of Melbourne's urban environment. https://www.melbourne.vic.gov.au/SiteCollectionDocuments/history-city-of-melbourne-urban-environment.pdf

Clean Energy Council (2009). Grid-Connected PV Systems System Design Guidelines for Accredited Designers

Compagnon R (2004). Solar and daylight availability in the urban fabric. Energy and Building, 36(4): 321–328

Deline C, Meydbray J, Donovan M, Forrest J (2012). Photovoltaic Shading Testbed for Module-Level Power Electronics. NREL Technical Report 5200-54876. Golden: National Renewable Energy Laboratory

Freitas S, Reinhart C, Brito M C (2018). Minimizing storage needs for large scale photovoltaics in the urban environment. Solar Energy, 159: 375–389

Frontini F, Bouziri S M, Corbellini G, Medici V (2016). S.M.O solution: an innovative design approach to optimize the output of BIPV systems located in dense urban environments. Energy Procedia, 91: 945–953

Horn B (2011). Maximizing Performance: Determining the Relative Influence of Key Design Elements on the Performance Grid Connected Solar Photovoltaic Systems in Geraldton, Western Australia. Thesis for the Master's Degree. Perth: Murdoch University

Jafarkazemi F, Saadabadi S A (2013). Optimum tilt angle and orientation of solar surfaces in Abu Dhabi, UAE. Renewable Energy, 56: 44–49

Jantsch M, Stoll M, Roth W, Kaiser R, Schmidt H, Schmid J (1991). The effect of tilt angle and voltage conditions on PV system performance an experimental investigation. In: Luque A, Sala G, Palz W, Dos Santos G, Helm P, eds. Tenth E.C. Photovoltaic Solar Energy Conference. Dordrecht: Springer, 431–434

Kaddoura T O, Ramli M A M, Al-Turki Y A (2016). On the estimation of the optimum tilt angle of PV panel in Saudi Arabia. Renewable & Sustainable Energy Reviews, 65: 626–634

Khahro S F, Tabbassum K, Talpur S, Alvi M B, Liao X, Dong L (2015). Evaluation of solar energy resources by establishing empirical models for diffuse solar radiation on tilted surface and analysis for optimum tilt angle for a prospective location in southern region of Sindh, Pakistan. International Journal of Electrical Power & Energy Systems, 64: 1073–1080

Loulas N M, Karteris M M, Pilavachi P A, Papadopoulos A M (2012). Photovoltaics in urban environment: a case study for typical apartment buildings in Greece. Renewable Energy, 48: 453–463

Melius J, Margolis R, Ong S (2013). Estimating Rooftop Suitability for PV: A Review of Methods, Patents, and Validation Techniques. NREL Technical Report 6A20-60593. Golden: National Renewable Energy Laboratory

Mohajeri N, Upadhyay G, Gudmundsson A, Assouline D, Kämpf J, Scartezzini J L (2016). Effects of urban compactness on solar energy potential. Renewable Energy, 93: 469–482

Mondol J D, Yohanis Y G, Norton B (2007). The impact of array inclination and orientation on the performance of a grid-connected photovoltaic system. Renewable Energy, 32(1): 118–140

National Centers for Environmental Information (2018). Magnetic declination. https://www.ngdc.noaa.gov/geomag-web/, 2018-6-2

Nguyen H T, Pearce J M (2012). Incorporating shading losses in solar photovoltaic potential assessment at the municipal scale. Solar Energy, 86(5): 1245–1260

NREL (2018). PVWatts calculator. http://pvwatts.nrel.gov/, 2018-5-20

Office of Best Practice Regulation (2016). Cost-benefit analysis guidance note. https://www.pmc.gov.au/resource-centre/regulation/cost-benefit-analysis-guidance-note, 2018-6-2

Redweik P, Catita C, Brito M (2013). Solar energy potential on roofs and facades in an urban landscape. Solar Energy, 97: 332–341

Rowlands I H, Kemery B P, Beausoleil-Morrison I (2011). Optimal solar-PV tilt angle and azimuth: an Ontario (Canada) case-study. Energy Policy, 39(3): 1397–1409

Sarralde J J, Quinn D J, Wiesmann D, Steemers K (2015). Solar energy and urban morphology: scenarios for increasing the renewable energy potential of neighbourhoods in London. Renewable Energy, 73: 10–17

Singh R, Banerjee R (2016). Impact of solar panel orientation on large scale rooftop solar photovoltaic scenario for Mumbai. Energy Procedia, 90: 401–411

State Government of Victoria (2018). Victorian feed-in tariff. https://www.energy.vic.gov.au/renewable-energy/victorian-feed-in-tariff, 2018-6-2

Talebizadeh P, Mehrabian M A, Abdolzadeh M (2011). Prediction of the optimum slope and surface azimuth angles using the genetic algorithm. Energy and Building, 43(11): 2998–3005

University of Melbourne (2008). Grid plan. http://www.emelbourne.net.au/biogs/EM00677b.htm, 2018-6-1

Wijeratne W M P U, Yang R J, Too E, Wakefield R (2018). Design and development of distributed solar PV systems: do the current tools work? Sustainable Cities and Society, 45: 553–578

Wong M S, Zhu R, Liu Z, Lu L, Peng J, Tang Z, Lo C H, Chan W K (2016). Estimation of Hong Kong's solar energy potential using GIS and remote sensing technologies. Renewable Energy, 99: 325–335

Woyte A, Nijs J, Belmans R (2003). Partial shadowing of photovoltaic arrays with different system configurations: literature review and field test results. Solar Energy, 74(3): 217–233

Yang R J, Carre A (2018). A feasibility study and assessment: distributed solar system in high-density areas. In: Rajagopalan P, Andamon M M, Moore T, eds. Energy Performance in the Australian Built Environment. Singapore: Springer, 167–181

Zomer C, Nobre A, Reindl T, Rüther R (2016). Shading analysis for rooftop BIPV embedded in a high-density environment: a case study in Singapore. Energy and Building, 121: 159–164

Zomer C, Nobre A, Yang D, Reindl T, Rüther R (2014). Performance analysis for BIPV in high-rise, high-density cities: a case study in Singapore. In: Proceedings of the 6th World Conference on Photovoltaic Energy Conversion, Kyoto, Japan, 1151–1152